Rapid genomic surveillance of SARS-CoV-2 in a dense urban community using environmental (sewage) samples

Genomic environmental surveillance of SARS-CoV-2 using sewage samples

Rajindra Napit[1,2], Prajwol Manandhar[1,2], Ashok Chaudhary[1], Bishwo Shrestha[1], Ajit Poudel[1,2], Roji Raut[1], Saman Pradhan[1,2], Samita Raut[1], Sujala Mathema[1], Rajesh Rajbhandari[1,2], Sameer Dixit[1], Jessica S. Schwind[3], Christine K Johnson[4], Jonna K Mazet[4], Dibesh Karmacharya[1,2 *]

[1] One Health Research Division, Center for Molecular Dynamics Nepal, Thapathali-11, Kathmandu 44600, Nepal

[2] Virology Division, BIOVAC Nepal Pvt. Ltd., Nala, Banepa, Nepal

[3] Department of Biostatistics, Epidemiology, and Environmental Health Sciences, Jiann-Ping Hsu College of Public Health, Georgia Southern University, Statesboro, GA 30458, USA

[4] One Health Institute, School of Veterinary Medicine, University of California, Davis, USA

*corresponding dibesh@cmdn.org, dibesh@biovacnepal.com

Abstract

Understanding disease burden and transmission dynamics in resource-limited, developing countries like Nepal is often challenging due to a lack of adequate surveillance systems. These issues are exacerbated by limited access to diagnostic and research facilities throughout the country. Nepal has one of the highest COVID-19 case rates (915 cases per 100,000 people) in South Asia, with densely-populated Kathmandu experiencing the highest number of cases. Swiftly identifying case clusters and introducing effective intervention programs is crucial to mounting an effective containment strategy. The rapid identification of circulating SARS-CoV-2 variants can also provide important information on viral evolution and epidemiology. Genomic-based environmental surveillance can help in the early detection of outbreaks before clinical cases are recognized, and identify viral micro-diversity that can be used for designing real-time risk-based interventions. This research aimed to develop a genomic-based environmental surveillance system by detecting and characterizing SARS-CoV-2 in sewage samples of Kathmandu using portable next-generation DNA sequencing devices. Out of 20 selected sites in the Kathmandu Valley, sewage samples from 16 (80%) sites had detectable SARS-CoV-2. A heat-map was created to visualize transmission activity in the community based on viral load intensity and corresponding geospatial data. Further, 41 mutations were observed in the SARS-CoV-2 genome. Some detected mutations (n=9, 2%) were novel and yet to be reported in the global database, with one indicating a frameshift deletion in the spike gene. We also observed more transition than transversion on detected mutations, indicating rapid viral evolution in the host. Our study has demonstrated the feasibility of rapidly obtaining vital information on community transmission and disease dynamics of SARS-CoV-2 using genomic-based environmental surveillance.

Introduction

In the past twenty years, several diseases caused by coronavirus have posed significant global health challenges- including Severe Acute Respiratory Syndrome (SARS, 2002), Middle East Respiratory Syndrome (MERS, 2012), as well as the current pandemic of COVID-19 [1,2]. COVID-19 is caused by a single-stranded, positive-sense RNA virus (SARS-CoV-2) which belongs to the *Coronaviridae* family [2]. The outbreak that was first detected in Wuhan (China) was declared a pandemic by the World Health Organization (WHO) on 11 March 2020, as it rapidly spread in over 114 countries [3]. As of January 14 (2021), over 108 million cases have been reported worldwide and have claimed over 2.3 million deaths [4]. In Nepal, there are 272,840 confirmed COVID-19 cases and 2055 deaths [5]. Gastrointestinal (GI) symptoms are often common in patients infected with SAR

S-CoV-2, with one hospital in the US reporting 70% of GI patients testing positive for coronavirus [6–9]. Although the primary source of transmission is through respiratory aerosol, studies have confirmed fecal shedding [10,11] and potential fecal-oral transmission of coronavirus [12,13]. Since SARS-CoV-2 is shed through feces and have also been detected in wastewater [14,15], detecting the virus in sewage and wastewater can serve as an early detection method for identifying communities with circulating virus in densely populated cities.

Environmental surveillance (ES) offers a complementary and more feasible approach to clinical disease surveillance. This approach provides unbiased information on a population level and detects viral shedding by symptomatic and asymptomatic patients [1,16], thus providing a snapshot of the outbreak over an entire sewage catchment area and an early indication of clinical cases in the area [17]. Because not all symptomatic patients get tested due to reluctance or lack of access

to tests, clinical samples are not a sensitive indicator of the occurrence of cases in a given area [18,19]. As experienced by many countries, clinical and community- based COVID-19 surveillance is expensive, technically challenging, and time-consuming, and therefore hard to implement in the manner needed to rapidly inform public health measures to contain the outbreak [10,20,21]. A longitudinal study conducted in Boston (USA) between March-April in 2020 showed a high correlation between environmental samples testing positive for the virus 4-10 days before symptoms presented in people in the sampled areas [16]. Wastewater sampling was as sensitive as stool sampling for viral detection during vaccine-derived poliovirus outbreaks in Cuba [22]. The versatility of environmental samples combined with the implementation of cheaper, user-friendly, and short turnaround sequencing tools such as MinION (Oxford Nanopore Technologies, UK) [23] will be invaluable in rapidly identifying viral strains and detecting clusters of infection going forward.

Whole-genome sequencing (WGS) of viral pathogens is frequently used in disease surveillance and monitoring, and the importance of genomic surveillance has been widely recognized as an important method of understanding viral evolution [24]. Portable and reliable sequencing tools such as MinION can play a crucial role in conducting genomic surveillance in a developing country like Nepal where access to high throughput DNA sequencing machines is limited. The pocket-sized and field-deployable, the next-generation sequencer has enabled real-time outbreak surveillance of several recent outbreaks of Zika, Ebola, and Lassa viruses [1]. Obtaining whole or partial genome sequences of the virus during outbreak is critical in understanding viral evolution and disease epidemiology, and can help design accurate diagnostic tests for rapidly evolving RNA viruses such as SARS-CoV-2 [25].

This study was conducted in some selected areas of Kathmandu (Nepal) to evaluate the effectiveness of SARS-CoV-2 detection and characterization from environmental samples using portable DNA sequencing technology (MinION). Studies in other countries have detected SARS-CoV-2 in environment samples collected from wastewater treatment plants (WWTP) [2,16,26–30]. However, Kathmandu has only one functional WWTP (out of five) and therefore, collecting all representative citywide sampling from WWTP is not possible. Since we had mapped sewage lines in some parts of the city for our ongoing surveillance of typhoid using environmental samples, we used the same sampling sites to conduct SARS-CoV-2 environmental surveillance. This cross-sectional study successfully detected, quantitated, and characterized the SARS-CoV-2 virus from environment samples collected from the wastewater outlets and utility holes within catchment areas, providing important information on the circulating strains of the virus in some communities of Kathmandu.

Materials and Methods

Sewage sample collection and processing

Much of the field sampling strategy was derived from our ongoing environmental surveillance work to determine the incidence of *Salmonella typhi* (the pathogen that causes Typhoid fever) in the Kathmandu valley, with an estimated population of over 4 million people [31]. As part of that study, we had comprehensively mapped sewage lines in the Lalitpur area of the Kathmandu valley. Also, we conducted field surveys to map out population size based on catchment areas. For our SARS-CoV-2 environmental surveillance, we used these sites and identified the catchment areas (n=20).

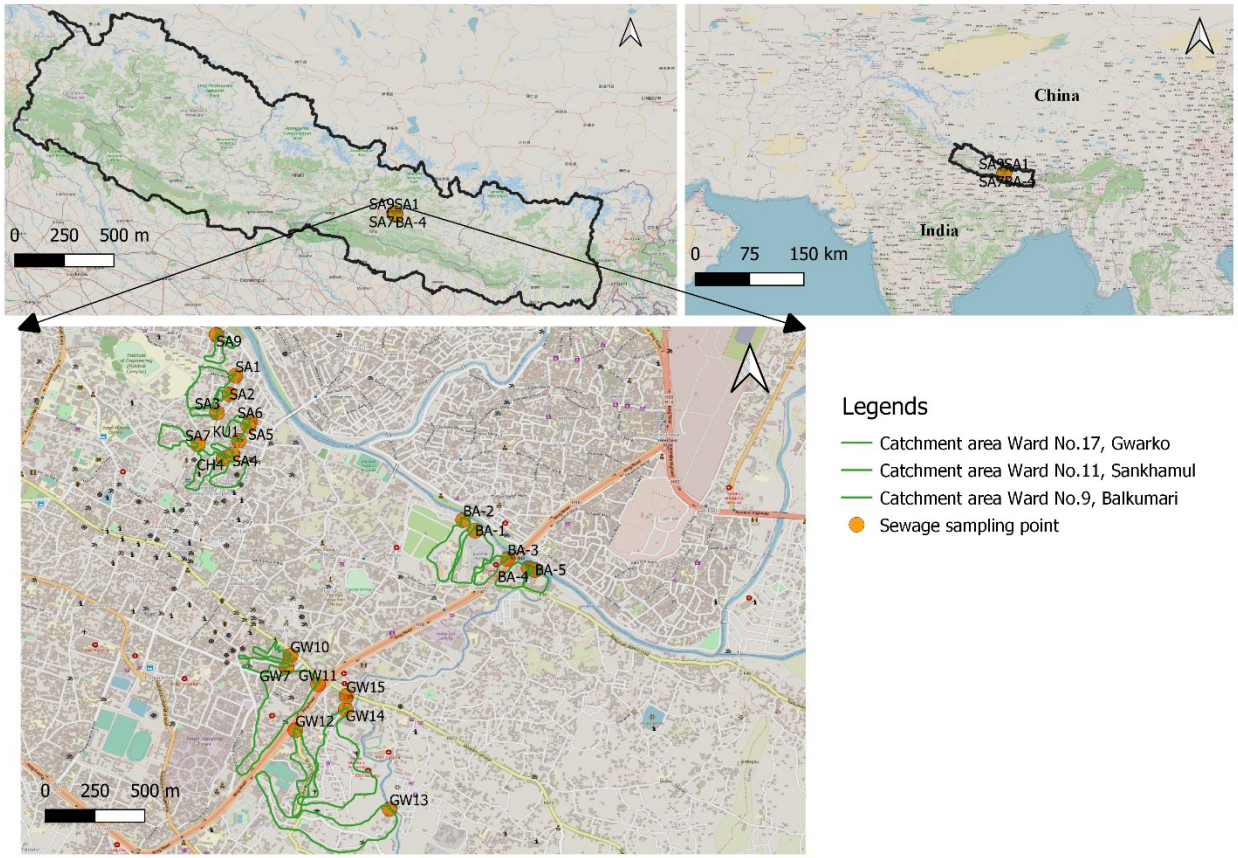

103

104 **Fig 1 Map of the sampling sites and respective catchment areas selected for the SARS-CoV-**
105 **2 environmental surveillance in the Kathmandu valley.** The sites were visualized in a map
106 using QGIS v3.16 [32] against a base map obtained from the Open Street Map [33].

107 The initial feasibility and optimization study (May 13-July 5, 2020) was carried out with sewage
108 samples collected around a hospital (Armed Police Force Hospital-APFH) with known COVID-
109 19 patients. Three different sites (Shankhamul (TH-1, N27.678734/E085.334175), Thapathali
110 (TH-2, N27.686754/E085.325203), and Teku (Te-3, N27.693163/E085.305504)) in the
111 Kathmandu valley were also selected based upon catchment area coverage and representative
112 population density.

Using an optimized protocol for detection and characterization of SARS-CoV-2, sewage samples were collected for the environmental and genomic surveillance (July 26- December 1, 2020) of three wards (Ward 9- Balkumari; Ward 11- Sankhamul/Jwagal, and Ward 17- Gwarko) located in the Lalitpur Metropolitan city of the Kathmandu valley (Nepal).

Sewage samples were collected using an automated robotic pump (Biobot Analytics Inc., Cambridge, USA). For protocol optimization, a total of 500ml of a composite (20.8 ml/hr) sample of 24 hours [16] was collected from the control site (APFH). But for the environmental surveillance, grab (50 ml) sample was preferred based upon outcome of optimization [34]. The probable reason for the consistent result in grab samples compared to the composite samples could be the dilution of viral particles by sewage discharge of non-viral peak hour [34]. The grab sewage samples were collected during the peak hour from 7:00AM to 9:00AM [35] based on the assumption that toilet activity and sewage discharge would be high during that time period.

The samples were transported immediately to our Kathmandu-based laboratory using cold chain for processing. Each sample was pasteurized at 60°C for 90 minutes in a water-bath [16] to inactivate any virus. Pasteurized samples were then subjected to differential centrifugation for virus segregation from sewage sludge by centrifuging at 3000 rpm for 30 minutes to pellet the bacterial cells and debris. The pellet was discarded, and the supernatant was precipitated for virus recovery using 15% PEG-6000 and 2% NaCl and gently shaken for 24 to 48 hours at 4°C [36]. The viral precipitates were then pelleted at 8000 rpm for 40 minutes and the pellet was re-

suspended in 400µl of SM buffer (Tris/NaCl/MgSO4) for further processing (Fig 2). The samples were handled in enhanced Biosafety Level 2 laboratory with full personal protective equipment.

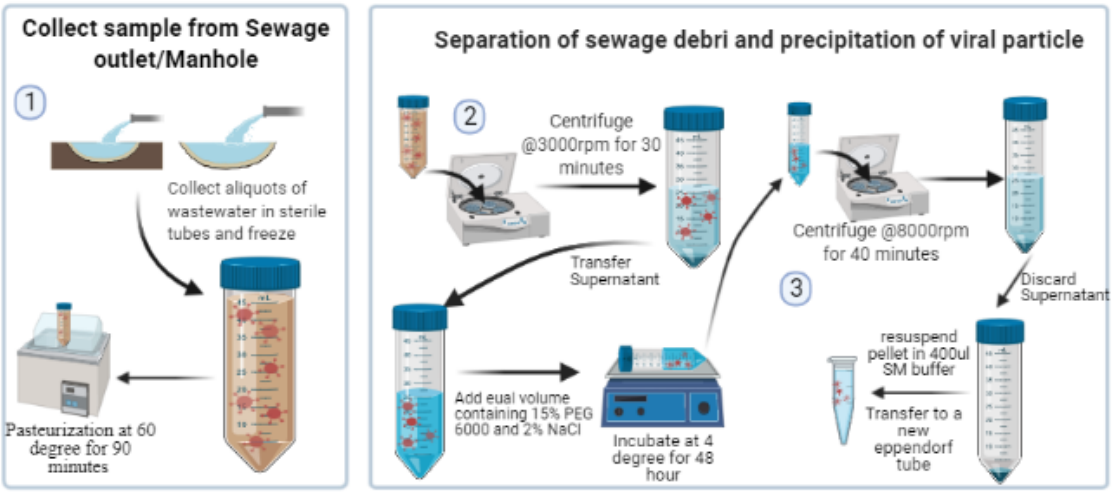

Fig 2 Environmental (sewage) sample processing for viral RNA extraction- 1) grab sewage samples collected, 2) differential centrifugation for virus isolation, 3) supernatant precipitation and virus recovery. This illustration was created using BioRender app [37].

SARS-CoV-2 detection using RT-PCR assay- Primary screening

We took samples from the sewage pipes of a selected hospital (Nepal Armed Police Hospital) with known admitted COVID-19 patients as a positive control site. Initially, regular diagnostic Real-Time polymerase chain reaction (PCR)-based assay (detecting envelope, nucleoprotein, and ORF1) was used to detect and quantify (sensitivity ~20 viral copies/ml) SARS-CoV-2.

We also used nested PCR-based assay (which detects all coronavirus, Fig 3) followed by meta-barcoding to increase the sensitivity significantly and confirm the presence of other circulating coronaviruses along with SARS-CoV-2.

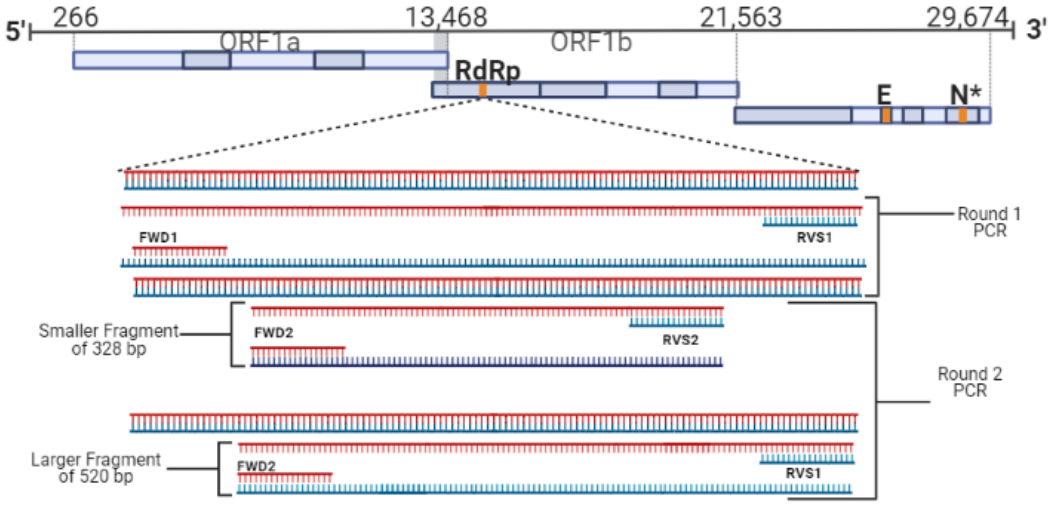

Fig 3 Nested PCR to detect corona virus- using two sets of primers (FWD1/RVS2 & FWD2/RVS1) two PCR amplicons (328bp and 520bp) were produced which were cleaned and sequenced using Flongle MinION. The obtained sequences were then BLAST analyzed in the NCBI database for viral taxonomic identification [38]. The images were created using BioRender app [37].

RNA was extracted from the viral suspension (200µl) (abGenix viral DNA and RNA Extraction Kit, AIT Biotech, Singapore) in an automated DNA and RNA extraction system (abGenixAIT Biotech, Singapore). SARS-CoV-2 was detected in sewage samples using Allplex™ RT-PCR SARS-CoV-2 Assay (Seegene Inc., Korea). The 5µl of extracted RNA was mixed with 10µl of qPCR mix consisting 2019-nCoV MOM (3µl), Real-time One-step Enzyme (1.2µl), 5X Real-time

One-step Buffer (3µl) and Nuclease free water (2.8µl) with manufacture recommended conditions- cDNA synthesis (50°C for 20 min); polymerase activation (95 °C for 15 min); PCR (45 cycles of denaturation at 94°C for 15 s, and annealing/extension at 58°C for 30 s). 2019-nCoV_RdRp (ORF1ab) Positive Control (cat. 10006897, IDT USA) obtained from the University of California-Davis with known copy number was used to build a standard curve to determine the viral load of SARS-CoV-2. The viral load quantitation data of each site were visualized geospatially using the Heat-map plugin in QGIS v3.16 [32]. The viral load data were first converted to log scale, and then attributes were used to generate the heat-map, which was plotted against a base map obtained from open street maps.

Coronavirus detection using meta-barcoding in MinION

To detect the presence of coronavirus other than SARS-CoV-2, we further screened RT-PCR negative samples with corona viral family-specific nested PCR modified on Quan et al. protocol using primers sets (FWD1/RVS2 &FWD2/RVS1) and producing 328bp and 520bp PCR amplicons [39] (Fig 3). 8µl of RNA template was mixed with 1µl of random hexamers and 1 µl of dNTPs and incubated at 65°C for 5 minutes. This mixture was combined with 10µl of synthesis mix consisting 10X RT (2µl), 25mM MgCl2 (4 µl), 0.1M DTT (2µl), RNase Out (1µl) and SSIII (1µl) (Superscript III (SSIII) cDNA synthesis kit, Invitrogen, USA). The final mixture was incubated at room temperature for 10 minutes, followed by incubation at 50°C for 50 minutes, and terminated at 85°C for 5 minutes. To remove any remnant RNA, the mixture was treated with 1µl of RNase H and incubated at 37°C for 20 minutes. The PCR amplicons were purified using a Montage Gel Purification kit (EMD Millipore Corp, USA) and sequenced using a portable next-generation sequencing device (Flongle MinION, Oxford Nanopore Technologies, UK). Nanoplot v1.30.1 [40] was used to check the quality of the raw nanopore fastq reads, and adapter sequences

were trimmed using Porechop v0.2.4 [41]. Length and quality filtering were performed using Filtlong v0.2.0 [42], with minimum length and q-score thresholds of 300bp and seven. The cleaned sequence reads were then de-novo assembled using Canu v2.0 [43] to generate contigs with an overlap parameter threshold of 100bp. The scaffolds generated were subjected to the Basic Local Alignment Search Tool (BLAST) [44] for taxonomic identification against locally downloaded GenBank database (Release 240, October 15 2020).

Whole-genome sequencing of SARS-CoV-2 using MinION

Library preparation and sequencing using MinION

Tiled amplicon sequencing was used to amplify the whole genome of SARS-CoV-2 using ARTIC PCR protocol [45]. This protocol has been widely adopted to sequence the entire genome of SARS-CoV-2 from clinical samples. With a set of 98 PCR primers, ARTIC PCR amplifies ~400bp amplicons spanning the SARS-CoV-2 genome with adjacent ~200bp overlaps. The sequencing library preparation is done by pooling these 98 primers in two pools and running two PCR reactions. We expect environmental samples to be highly degraded, and hence this protocol suits well for our study as smaller-sized amplicon increases the success of whole-genome amplification.

25µl reaction volume from each PCR pool were prepared containing 12.5µl Ampligold 360 2X MM, 3.6µl of primers and 2µl template cDNA. The PCR conditions were: 95°C for 30 secs followed by 45 cycles of 95°C for 15 secs, 63°C for 5 mins. The ARTIC PCR amplicons were further cleaned (AMPure bead, Agencourt, Beckman Coulter, USA) and quantified (Qubit 3, Invitrogen Thermofisher Scientific, USA). The PCR amplicons were pooled into a single tube at an equimolar concentration of 100fm. Native barcodes were assigned for each sample using Native barcoding Expansion kit (EXP-NBD104) and ligation sequencing kit (SQK-LSK109) and run in Flongle Flowcell using MinION (Oxford Nanopore, UK). Up to 14 samples were multiplexed in three FLO-FLG001 Flongle flow cells (R9.4.1) and sequenced on MinION Mk1B device in three different sequencing runs.

Bioinformatics workflow for consensus genome sequence generation

MinKNOW software (Oxford Nanopore, UK) was used to monitor sequencing run, collect the raw data, and perform real-time base calling. The RAMPART v1.2.0 [46] software package developed by the ARTIC network was used to visualize read mapping and genome coverage in real-time for each barcode.

Data analysis was done using the ARTIC pipeline v1.1.3 [47] of the ARTIC network's nanopore bioinformatics protocol [48]. Base-calling was performed in real-time by Guppy v4.4.0 (Oxford Nanopore, UK) integrated within MinKNOW v20.10.3 (Oxford Nanopore, UK) using high-accuracy base calling mode in Thinkpad P72 Mobile Workstation (Lenovo, USA), which generated fast5 and fastq reads.

De-multiplexing was performed by Guppy using strict parameters requiring barcodes (indexes) at both ends of the reads and quality filtering (qscore threshold 7) was performed within MinKNOW platform. This generated pass and fail reads for each barcode in individual directories.

Further filtering of read length was performed using the ARTIC pipeline with *guppyplex* option considering parameters of certain threshold length only (range 400 bp -700 bp) that removed obvious chimeric reads.

The processed reads were subjected to mapping, aligning, variant and consensus calling using the ARTIC pipeline with the *minion* option. The reads were mapped against the SARS-CoV-2 reference (NC_045512/MN908947) using the Minimap2 v2.17 [49]. The aligned read files were sorted using SAMtools v1.11 [50] to obtain coverage data and a consensus sequence.

Whole-genome sequencing of SARS-CoV-2 using MiSeq

Using identical ARTIC amplicons, the first two positive samples from the study were sequenced in MiSeq (Illumina, USA) platform. The amplicons were cleaned (AMPure bead, Agencourt, Beckman Coulter, USA), and a library was prepared using the Nextera XT library preparation kit [24]. The data was processed and a consensus sequence was generated using a nextflow-based SARS-CoV-2 Consensus Genome Pipeline developed by Chan Zuckerberg Biohub [51].

Geo-spatial mapping of identified variants of SARS-CoV-2

Identification of known and novel mutations in the obtained whole-genome sequences of SARS-CoV-2 was performed using a CoV-GLUE web application-based bioinformatics tool [52]. This tool is based on a GLUE data-centric bioinformatics environment that analyzes nucleotide variations in user-submitted sequences of SARS-CoV-2, enabled by data from EpiCoV of GISAID database. The tool compares and analyses the sequences against the reference sequence of SARS-CoV-2 and generates lists of amino acid replacements and coding region indels. The mutation table data obtained from CoVGlue was formatted to contain column names as follows; “sample", "gene", "variant_class", "amino.acid.change”. Once the data has been formatted, it was imported to R studio and were processed using plugin GenVisR to generate mutation landscape plot (Waterfall plot) [53].

The tool also provides a lineage based on Pangolin classification of SARS-CoV-2 clades and its LWR (likelihood weight ratio) score, which approximates confidence level of clade assignments based on quality of the submitted sequence. The distribution of lineages across the sampling sites were visualized in a map using QGIS v3.16 [32] against a base-map obtained from the Open Street map [33].

Results

Optimization of protocol for the detection of SARS-CoV-2 and other coronaviruses in sewage samples

Four preliminary sites were selected (Armed Police Force Hospital (APFH), Thapathali (TH1), Shankhamul (TH2) and Teku (Te3)) for the initial protocol development and optimization. Along with SARS-CoV-2, we also detected other coronaviruses, including Human coronavirus 229E, Duck-dominant coronavirus, Dromedary camel coronavirus HKU223, and Rat coronavirus, in two preliminary sites (TH1 and Te3) (S1 Table).

Whole-genome sequencing of SARS-CoV-2 using MinION and MiSeq

Whole-genome sequencing data of detected SARS-CoV-2 were obtained using MinION and MiSeq from two different sites (TH1 and Te3). The result showed a slight difference in genome coverage and contigs recovered from both the platforms. We observed slightly higher genome fraction coverage on MiSeq than on MinION. In one of the samples (TH1), MiSeq produced relatively high (47.2%) genome fragment sequences compared to MinION (32.2%). A similar result was observed in the other sample (Te3), with MiSeq producing around 42.9% sequences compared to 31.1% from MinION (Table 1).

Table 1 MinION sequencing run details and run statistics

	First Run	Second Run	Third Run
Number of samples	2	6	6
Total raw reads	693,554	312,602	128,107
Total mapped reads	414,002	253,168	102,011
Median reads length	482	494	477
Passed reads	433,024	258,256	104,856
Genome fraction (%) at >20x	33 to 36	32.3 to 51.9	28.2 to 71.8
Run duration hours	23.55	18.47	14.89

CoVGlue analyses [52] of consensus genomic sequences from both the sequencing platforms indicated the presence of the same Pangolin lineage (**B.1**). Major mutations were plotted to visualize and differentiate key differences between MiSeq and MinION using the GenVisR tool in R studio Version 1.4.1103. We detected **D614G** which is the defining mutation of the G clade [54]. MiSeq did detect more mutations than MinION (Fig 4). This finding can be due to greater sequencing depth (1 million reads) obtained in MiSeq than in MinION using Flongle (378,000

280 reads). Despite shallow sequencing depth in MinION, both platforms successfully detected major
281 mutations and provided adequate sequencing coverage data for lineage identification [55].

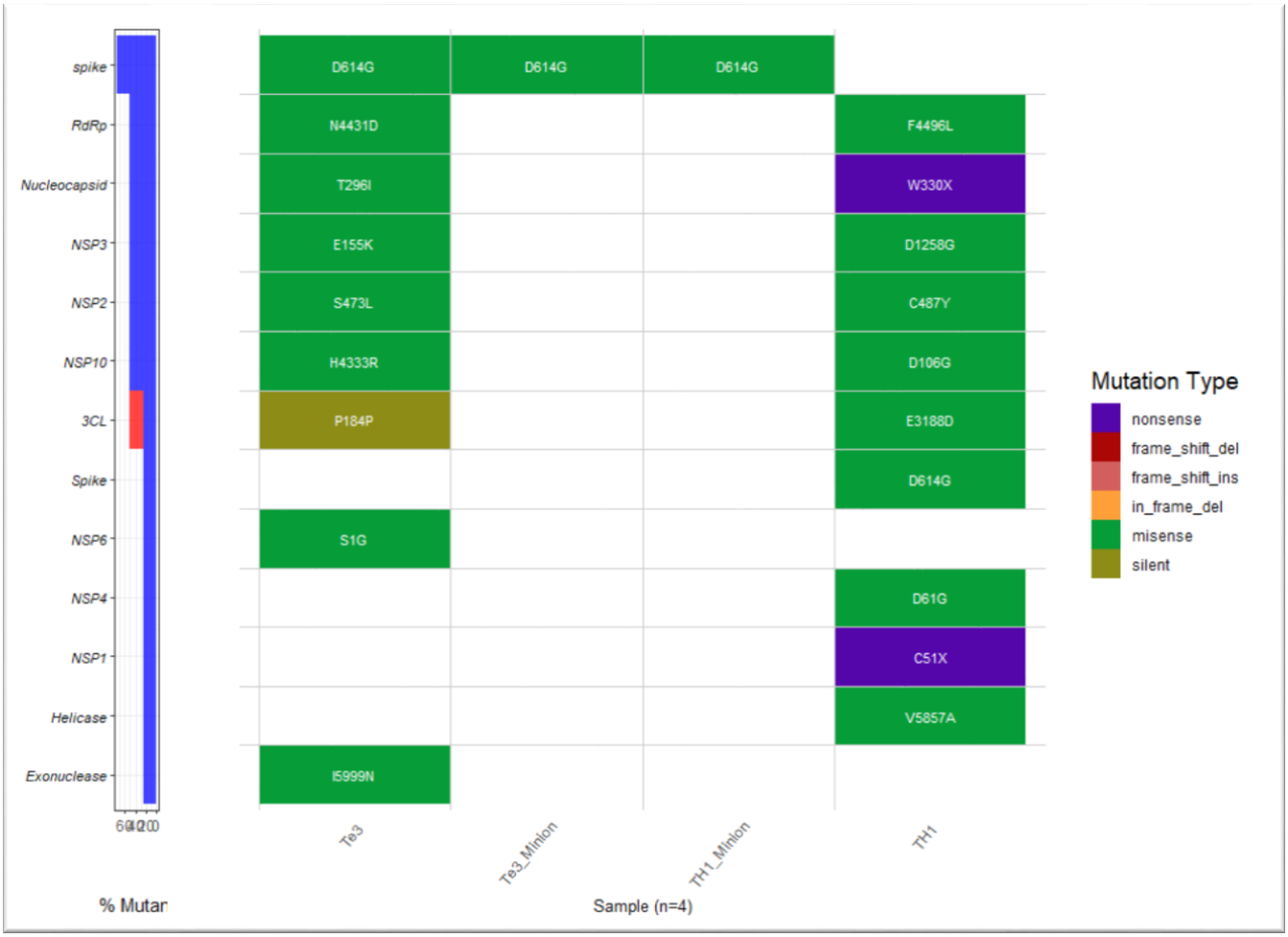

282 **Fig 4 Detected mutations in the environmental samples using MinION and MiSeq**. In this
283 waterfall plot, rows represent genes with key detected mutations with the columns' corresponding
284 samples. Based on the weight of mutation type (orderly displayed in the legend with **nonsense**
285 having greater impact and **silent** having the least impact on gene expression), only major mutations
286 in a particular gene in each sample are displayed. Samples from two sites (TH1 and Te3) were
287 sequenced using MiSeq (TH1 and Te3), and MinION (TH1_Minion and Te3_Minion) (Waterfall
288 plot created using CovGlue and GenVisR [56] on R studio version 1.4.110).

289

SARS-CoV-2 genomic-based environmental surveillance with sewage samples

Out of 20 sites, sewage samples from the 16 sites had detectable SARS-CoV-2 (S2 Table). A heat-map of all these 16 SARS-CoV-2 positive sites was created based on viral load intensity and corresponding geospatial data. With a relatively large number of sampling points, dense populations and detected viral load (295 copies/ml), Ward 11 (est. pop=4632) is colored dark in the heat- map. Although Ward 17 (est. pop=9500 people) had the most intense viral load (242,000 copies/ml), the sampling points do not cover the entire area, and hence lightly colored in the heat-map than Ward 11. In Ward 9 (est. pop= 2791 people), we did not detect SARS-CoV-2 (Fig 5).

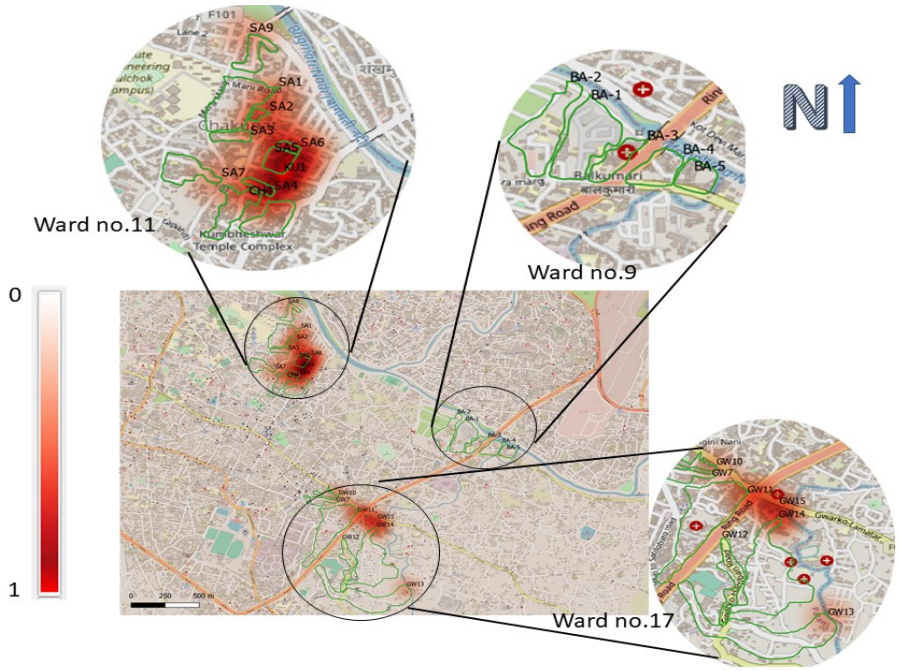

Fig 5 SARS-CoV-2 heat-map based on viral load intensity from sites with detectable virus. Heat-map of three sampled wards (11, 9 and 17) of the Lalitpur Municipality (Kathmandu valley)

303 with SARS-CoV-2 presence and its viral load intensity in sewage samples. The map was created
304 using QGIS v3.16 [32] with base-map from the Open Street Map [33].

305 Whole-genome sequencing of SARS-CoV-2 on MinION

306 Only samples from 14 sites (GW11, SA2, SA7, CH4, KU1, SA5, GW10, GW13, GW14, SA6,
307 SA4, SA9, GW12 and GW15) yielded PCR amplicons using ARTIC primers, of which only 12
308 samples (GW11, SA2, SA7, CH4, KU1, SA5, GW14, SA6, SA4, SA9, GW12 and GW15) had
309 enough quantifiable PCR products (S3 Table, S4 Table) and were tagged with Native Barcode
310 from NBD01 to NBD012 [24]. The consensus genomic sequences of SARS-CoV-2 have been
311 submitted to National Center for Biotechnology Information (NCBI) GenBank (accession no.
312 MW739929-MW739930). MinION sequencing was performed with 6 samples at a time, and run
313 data is shown in Table 1.

314 All of the consensus sequences obtained from MinION were compared against the reference
315 sequence (accession no. MN908947.3) using the CovGlue web application. **B.1** (16.7%), **B.1.36**
316 (33.3%) and **B.1.1** (50.0%) were identified as circulating lineages of SARS-CoV-2 in the
317 environmental (sewage) samples (Fig 6).

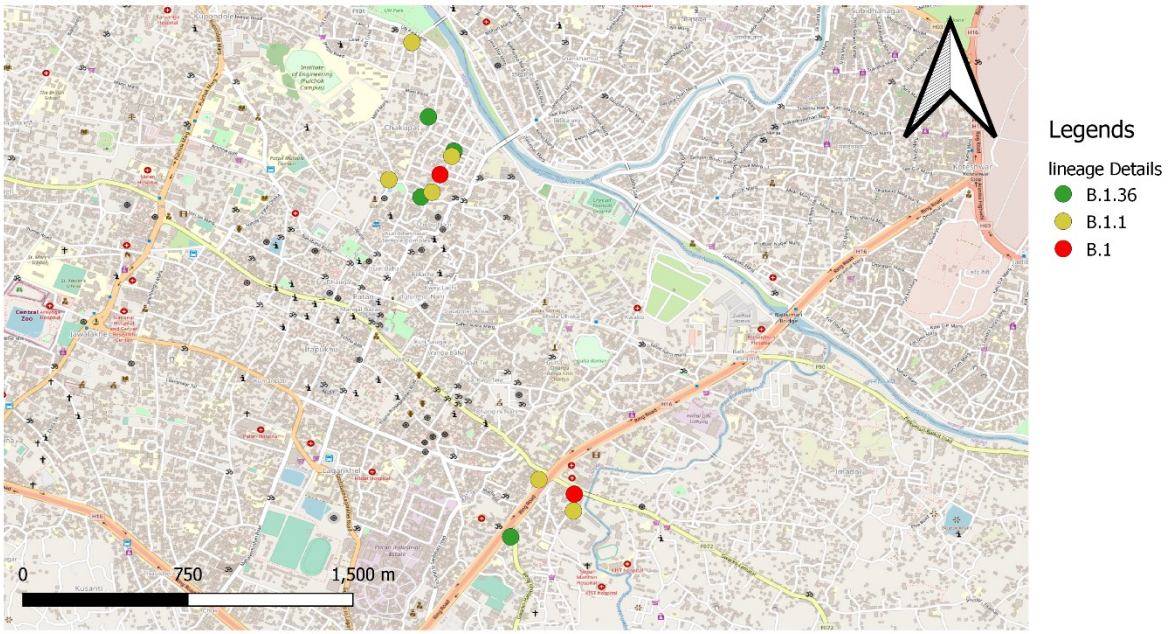

318

319 **Fig 6 Geographic distribution of the detected SARS-CoV-2 Pangolin lineages** *[56]* **in the**
320 **environmental samples from CovGlue submission**. Three wards of Lalitpur Municipality
321 (Kathmandu valley) with a distribution of detected SARS-CoV-2 and its lineages in sewage
322 samples (Created using QGis 3.16 using Open Street Map [33]).

323 SARS-CoV-2 evolution trend

324 Transition-Transversion mutation summary was visualized with a waterfall plot and created with
325 GenVisR [55] (Fig 7). Nucleotide mutation summary of all the samples showed a greater frequency
326 of transition (G>A (G>U) or C>T) in most of the samples, followed by transversion (G>T or C>A
327 (C>U). Overall transition seems to have occurred in greater frequency than transversion
328 (transition=57.5%, transversion=42.4%); and A>C or T> G transversion is rarely detected (16.4%)
329 (Fig 8). A higher number of transitions in detected mutations indicate a rapid evolution of SARS-
330 CoV-2 in the host [57].

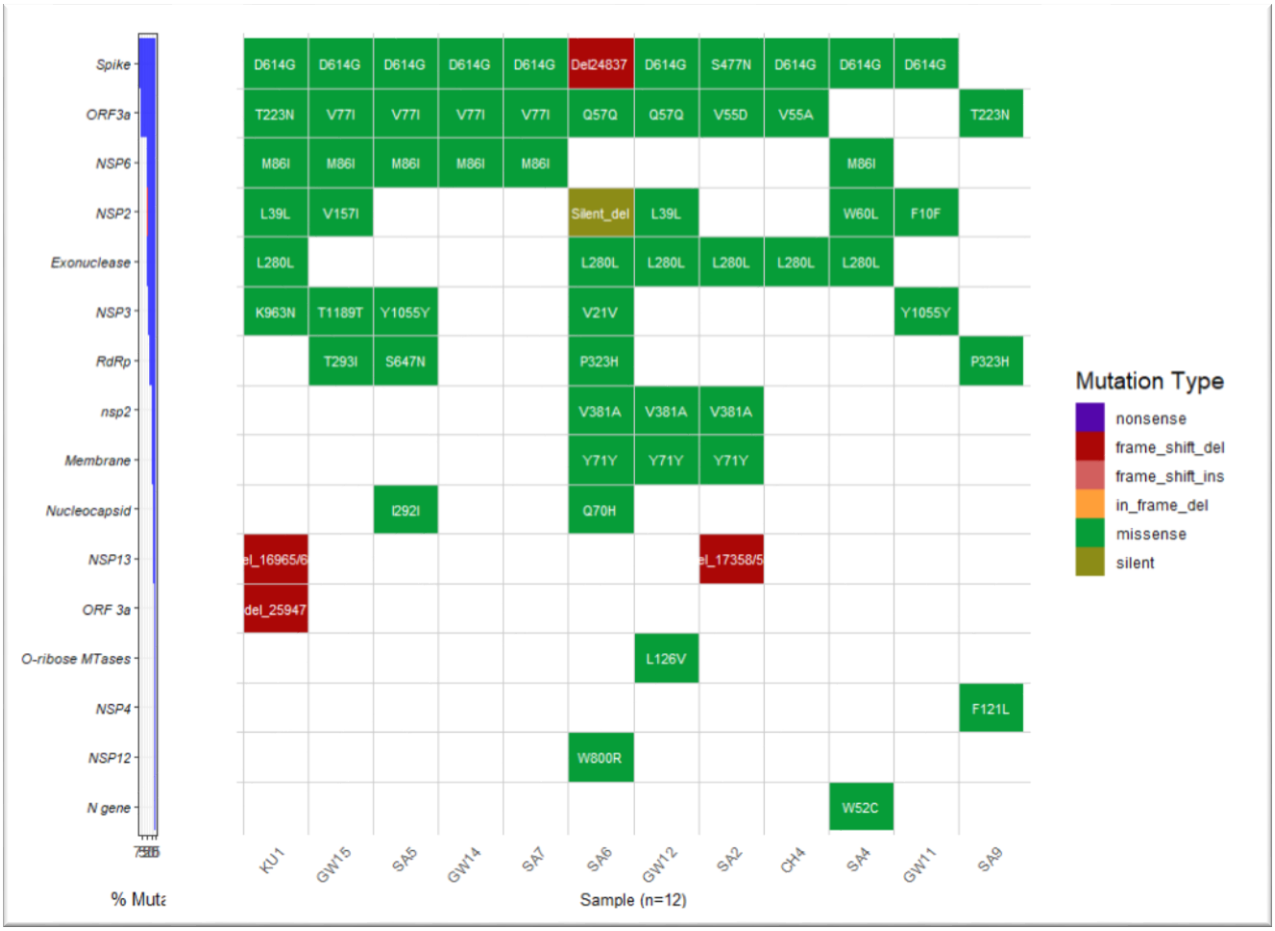

331

332 **Fig 7 Detected SARS-CoV-2 genes and their associated mutations.** Rows represents genes with

333 major mutations detected while column represents sample, a waterfall plot was created based upon

334 the weight of mutation type with nonsense having greater impact and silent having the least impact
335 on gene expression. Created using CovGlue and GenVisR [56] on R studio version 1.4.110.

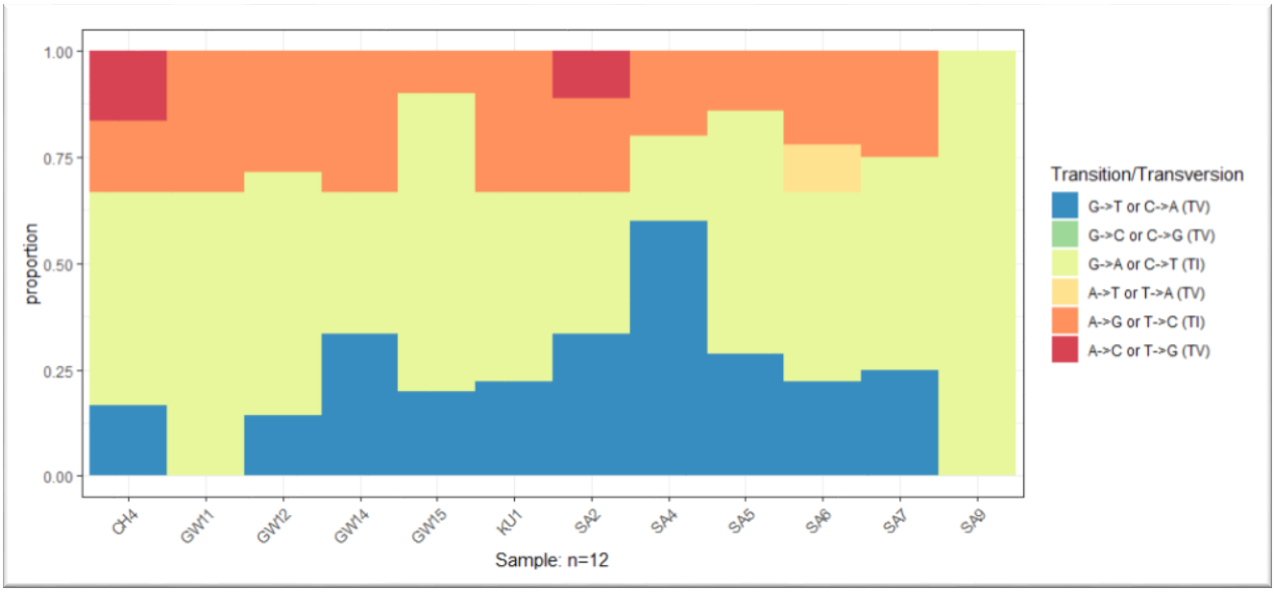

336

337 **Fig 8 Transition-Transversion mutation summary plot** from the mutation table detected by
338 CovGlue using GenVisR [55] on R studio version 1.4.1103, showing various genes with detected
339 mutations.

340 A total of 41 distinct mutations were detected across the SARS-CoV-2 genome with nine novel
341 mutations - six due to deletion. Of all the deletions detected, two were non-codon aligning
342 deletions, whereas the rest were frameshift deletion, including one in the spike gene (Fig 7, Fig 9).
343 Major mutations were detected in spike, ORF3a, NSP6, and Exonuclease genes of SARS-CoV-2.
344 **D614G** and **S477N** mutations were detected in the spike gene. Other genes with frameshift deletion
345 include **NSP13** and **ORF3a** gene and one silent deletion on the **NSP2** gene (Fig 7, Fig 9).

346

347 **Fig 9 Detected mutations and their frequencies in the SARS-CoV-2 genome from**
348 **environmental samples (n=12).** The frequency of detected mutations on the corresponding genes
349 is labeled at the top of the chart with height representing the frequency level. The lables on the X-
350 axis were extracted from GISAID[58].

351 The novel mutations with amino acid changes were detected on the **W800R**, **W60L** and **W52C** in
352 **NSP12**, **NSP2** and **N** genes. Among these three detected mutations, two were from the same
353 sample (**SA4**), and one was from **SA6** collected from different sampling sites from the same ward.

354

Discussion

As demonstrated by its successful application in the global efforts to eradicate poliovirus [24], ES can be an important supplement to clinical surveillance. In particular, ES can contribute to several critical areas, such as characterizing regional diversity in areas without clinical surveillance, mapping geographic micro-diversity to inform risk-based interventions, early detection of outbreaks before clinical presentation, and advancing real-time assessment of interventions to inform need for additional public health measures [24]. Compared to clinical surveillance, ES can be inexpensive and fast, but this approach has yet to be fully validated as a viable option for estimating disease burden in a field setting.

Rapid detection of SARS-CoV-2 in environmental samples (such as sewage) and viral strain characterization using portable genomic tools provide important information on disease distribution at a community level [24]. Such data can help identify transmission hotspots in urban and rural communities and provide information on circulating strains of viruses, an essential consideration for vaccination programs. We have optimized a system of detecting the virus from sewage samples, and based on viral load, we have constructed a heat-map of SARS-CoV-2 in the selected areas of the Kathmandu valley. In resource-limited, developing countries like Nepal, access to tools and technologies required to perform genomic-based detection and surveillance can be limited. This feasibility study has demonstrated that ES based on sewage samples using highly sensitive nested PCR combined with portable next-generation sequencing technology can provide adequate sensitivity, specificity, and sequencing depth to detect, quantify, and characterize SARS-CoV-2 accurately.

Whole-genome sequencing of the SARS-CoV-2 was obtained using ARTIC primers in two popularly used next-generation sequencing platforms (MiSeq (Illumina, USA) and MinION (Oxford Nanopore, UK)). One of our main objectives was to explore the feasibility of using a portable sequencing platform in Nepal. Using the same protocol, the sequencing data obtained from both these platforms were analyzed, and the results obtained were almost identical, demonstrating the suitability of using portable sequencing devices such as MinION to characterize viral (SARS-CoV-2) strains. However, with CoVGlue analysis, we were able to detect more variants (mutations) in Illumina MiSeq than ONT MinION using Flongle flowcell. We can use Flongle (MinION) for screening for rapid surveillance, and further detailed analysis can be done either on MiSeq or SpotON Flowcell (MinION).

In our ES samples, we were also able to detect other coronaviruses such as human coronavirus 229E, a known cause of the common cold with global distribution [24,59]. The presence of duck dominant coronavirus and rodent coronavirus in sewage suggests an abundant mixture of various coronaviruses originating from other species. A diversity of coronaviruses in sewage samples highlights the potential for emerging coronaviruses among species in close proximity in the urban setting, especially given the propensity for coronaviruses to recombine [60].

Out of 20 different sampled sites, 16 had SARS-CoV-2 present. The heat-map generated based on the intensity of viral load correlated well with the catchment area and population size (Fig 5). Analyzing enough sampling points can provide a good picture of circulating viruses in a community. Further studies can be designed to look into incidence estimation in communities and correlate that with available clinical data.

The obtained consensus genome sequences of SARS-CoV-2 from the sewage samples identified **B.1**, **B.1.36** and **B1.1** as circulating lineage. The lineage **B.1** was a strain circulating in the United States of America (46.0%), United Kingdom (13.0%), Canada (5.0%), Spain (4.0%), and France (4.0%); and was involved in the Italian outbreak [24,61]. **B.1.1** was also widely circulating around the globe (United States of America (27.0%), United Kingdom (22.0%), Canada (6.0%), Germany (6.0%), and Netherlands (5.0%)) and is cited as a European lineage [61]. Lineage **B.1.36** was the predominant strain circulating in the United States of America (94.0%), and is known as a USA lineage[61]. Whole-genome data of SARS-CoV-2 from 14 clinical samples have been sequenced at our facility for the Nepal Health Research Council (Government of Nepal). Data are publicly available in the GISAID database [24]. Among these, three samples originate from the Kathmandu valley, and identified lineages include **B.1.36** and **B.1.130**. The detected SARS-CoV-2 lineages (**B.1, B.1.1, B.1.36**) and key mutations such as **D614G** in the clinical samples were also circulating in the sewage samples.

Among the detected mutations, the majority were transitions that provide a snapshot of the evolutionary dynamics of SARS-CoV-2 in the host. Few novel mutations with possible clinical significance were also detected- such as frameshift and silent deletion mutations in **S**, **NSP13**, **ORF3a,** and **NSP2** genes. These novel mutations are yet to be reported in the global database, and their functional characterizations are further required. For example, frameshift deletion in the S gene could have important significance in clinical and epidemiological frames. The D614G (in S gene) was spontaneously detected in almost every sample, a defining mutation for the G clade [54]. This particular mutation is associated with increased infectivity of SARS-CoV-2 [23]. Another detected mutation, S477N (in S gene), has been reported to increase the binding affinity of the virus to the host's angiotensin-converting enzyme 2 (ACE-2) receptor giving higher

transmission capability [62,63]. Similarly, novel missense mutations detected in **NSP12**, **NSP2,** and **N** genes from sites in the same Ward indicated ongoing viral circulation in the community. These inferences tell us that the virus is spreading rapidly throughout the community, which provides the virus opportunities for rapid evolution. Such a scenario creates an environment for the emergence of new variants, which was also the reason behind the origins of emerging variants in the UK (B.1.1.7), South Africa (B.1.351), and South America (P.1) [64]. This finding also highlights the mandates for genomic surveillance to track viral evolution and emerging variants.

Three major vaccines (Pfizer-BioNTech, Moderna, and Oxford-AstraZeneca) approved by the WHO target spike protein to produce neutralizing antibodies against SARS-CoV-2 [65]. The detection of circulating viral variants through genomic surveillance has become more critical than ever to evaluate the efficacy of the vaccine against the evolving virus. For this reason, genomic surveillance is gradually being conducted in many developed countries, with the United Kingdom contributing actively to the global genomic database of SARS-CoV-2 [66]. However, developing countries are still struggling to understand COVID-19 incidences and transmission due to a lack of genomic laboratory capabilities. Genomic surveillance in environmental samples could be a possible solution for resource-strapped countries to identify and estimate SARS-CoV-2 presence at a community level and determine the circulating strains of the virus, which could be used to select the most appropriate vaccine.

Acknowledgments

We would like to thank the Mayor's Office of the Lalitpur Metropolitan City for providing us with permit and encouraging us to conduct this research. We would like to thank Professor Eric Alm and Dr. Noriko Endo of BIOBOT (USA) for providing composite sampling robots. We would also like to express our gratitude to the One Health Institute of the University of California-Davis and the USAID-funded PREDICT project for providing us with laboratory resources. Whole-genome sequencing was done at the Intrepid Nepal Genomic Center- some of our work was partially funded by the Australian Development Agency and PSI grant (the Netherlands). We would like to thank all these agencies for their support. And finally, we would like to thank everyone at Intrepid Nepal Pvt Ltd, Center for Molecular Dynamics Nepal and BIOVAC Nepal for their tireless work, even during nationally enforced lockdown in Nepal.

Figure Captions

Fig 1 Map of the sampling sites and respective catchment areas selected for the SARS-CoV-2 environmental surveillance in the Kathmandu valley. The sites were visualized in a map using QGIS v3.16 [32] against a base map obtained from the Open Street Map [33].

Fig 2 Environmental (sewage) sample processing for viral RNA extraction- 1) grab sewage samples collected, 2) differential centrifugation for virus isolation, 3) supernatant precipitation and virus recovery. This illustration was created using BioRender app [37].

Fig 3 Nested PCR to detect corona virus- using two sets of primers (FWD1/RVS2 & FWD2/RVS1) two PCR amplicons (328bp and 520bp) were produced which were cleaned and sequenced using Flongle MinION. The obtained sequences were then BLAST analyzed in the NCBI database for viral taxonomic identification [38]. The images were created using BioRender app [37].

Fig 4 Detected mutations in the environmental samples using MinION and MiSeq. In this waterfall plot, rows represent genes with key detected mutations with the columns' corresponding samples. Based on the weight of mutation type (orderly displayed in the legend with **nonsense** having greater impact and **silent** having the least impact on gene expression), only major mutations in a particular gene in each sample are displayed. Samples from two sites (TH1 and Te3) were sequenced using MiSeq (TH1 and Te3), and MinION (TH1_Minion and Te3_Minion) (Waterfall plot created using CovGlue and GenVisR [56] on R studio version 1.4.110).

Fig 5 SARS-CoV-2 heat-map based on viral load intensity from sites with detectable virus. Heat-map of three sampled wards (11, 9 and 17) of the Lalitpur Municipality (Kathmandu valley)

with SARS-CoV-2 presence and its viral load intensity in sewage samples. The map was created using QGIS v3.16 [32] with base-map from the Open Street Map [33].

Fig 6 Geographic distribution of the detected SARS-CoV-2 Pangolin lineages *[56]* **in the environmental samples from CovGlue submission**. Three wards of Lalitpur Municipality (Kathmandu valley) with a distribution of detected SARS-CoV-2 and its lineages in sewage samples (Created using QGis 3.16 using Open Street Map [33]).

Fig 7 Detected SARS-CoV-2 genes and their associated mutations. Rows represents genes with major mutations detected while column represents sample, a waterfall plot was created based upon the weight of mutation type with nonsense having greater impact and silent having the least impact on gene expression. Created using CovGlue and GenVisR [56] on R studio version 1.4.110.

Fig 8 Transition-Transversion mutation summary plot from the mutation table detected by CovGlue using GenVisR [55] on R studio version 1.4.1103, showing various genes with detected mutations.

Fig 9 Detected mutations and their frequencies in the SARS-CoV-2 genome from environmental samples (n=12). The frequency of detected mutations on the corresponding genes is labeled at the top of the chart with height representing the frequency level.

Table Caption

Table 1 MinION sequencing run details and run statistics

Supporting Information Captions

S1 Table: Blast result analysis of Coronavirus origin from sewage samples of Pilot phase study

S2 Table: Real time PCR data, viral load and population distribution of different sites. Amplified genes- envelope (E), internal control (house-keeping gene, IC), RdRp and nucleoplasmid (N) genes.

S3 Table: AMPure bead clean up and DNA quantification data of pool1 & pool2 artic PCR products in positive sewage samples before Indexing (Pilot study)

S4 Table: AMPure bead clean up and DNA quantification data of pool1 & pool2 ARTIC PCR products in positive sewage samples before indexing

Data Availability Statement: The data used to support the findings of this study are included within the article. Accession numbers mentioned in this study are- MW739929 & MW739930.

Funding: This research project was funded by BIOVAC Nepal and Intrepid Nepal Pvt. Limited. With partial funding support from the PREDICT project, Australian Development Agency and PSI grant from the Government of the Netherlands.

Competing interests: The authors have declared that no competing interests exist.

511 **References**

512 1. Hourdel V, Kwasiborski A, Balière C, Matheus S, Batéjat CF, Manuguerra J-C, et al. Rapid Genomic
513 Characterization of SARS-CoV-2 by Direct Amplicon-Based Sequencing Through Comparison of
514 MinION and Illumina iSeq100TM System. Frontiers in microbiology. 2020.

515 2. Venugopal A, Ganesan H, Raja SSS, Govindasamy V, Arunachalam M, Narayanasamy A, et al. Novel
516 Wastewater Surveillance Strategy for Early Detection of COVID–19 Hotspots. Current Opinion in
517 Environmental Science & Health. 2020.

518 3. Medema G, Heijnen L, Elsinga G, Italiaander R, Brouwer A. Presence of SARS-Coronavirus-2 in
519 sewage. MedRxiv. 2020.

520 4. COVID-19 Data Repository by the Center for Systems Science and Engineering (CSSE) at Johns
521 Hopkins University. In: GitHub [Internet]. [cited 31 Jan 2021]. Available:
522 https://github.com/CSSEGISandData/COVID-19

523 5. -44_weekly-who-nepal-situation-updates.pdf. Available: https://cdn.who.int/media/docs/default-
524 source/nepal-documents/novel-coronavirus/who-nepal-sitrep/-44_weekly-who-nepal-situation-
525 updates.pdf?sfvrsn=f2d844f4_13

526 6. Bolia R, Ranjan R, Bhat NK. Recognising the Gastrointestinal Manifestation of Pediatric Coronavirus
527 Disease 2019. The Indian Journal of Pediatrics. 2020. pp. 1–2.

528 7. Gao QY, Chen YX, Fang JY. 2019 novel coronavirus infection and gastrointestinal tract. Journal of
529 digestive diseases. 2020. pp. 125–126.

530 8. Nobel YR, Phipps M, Zucker J, Lebwohl B, Wang TC, Sobieszczyk ME, et al. Gastrointestinal
531 symptoms and coronavirus disease 2019: a case-control study from the United States.
532 Gastroenterology. 2020. pp. 373-375. e2.

533 9. Papa A, Covino M, Pizzolante F, Miele L, Lopetuso L, Bove V, et al. Gastrointestinal symptoms and
534 digestive comorbidities in an Italian cohort of patients with COVID-19. European review for medical
535 and pharmacological sciences. 2020. pp. 7506–7511.

536 10. Wang X-W, Li J-S, Guo T-K, Zhen B, Kong Q-X, Yi B, et al. Concentration and detection of SARS
537 coronavirus in sewage from Xiao Tang Shan Hospital and the 309th Hospital. Journal of virological
538 methods. 2005. pp. 156–161.

539 11. Yam W, Chan K, Poon L, Guan Y, Yuen K, Seto W, et al. Evaluation of reverse transcription-PCR
540 assays for rapid diagnosis of severe acute respiratory syndrome associated with a novel coronavirus.
541 Journal of clinical microbiology. 2003. pp. 4521–4524.

542 12. Yeo C, Kaushal S, Yeo D. Enteric involvement of coronaviruses: is faecal–oral transmission of
543 SARS-CoV-2 possible? The lancet Gastroenterology & hepatology. 2020;5: 335–337.

544 13. Zhang J, Wang S, Xue Y. Fecal specimen diagnosis 2019 novel coronavirus–infected pneumonia.
545 Journal of medical virology. 2020. pp. 680–682.

14. Wang X-W, Li J-S, Jin M, Zhen B, Kong Q-X, Song N, et al. Study on the resistance of severe acute respiratory syndrome-associated coronavirus. Journal of virological methods. 2005. pp. 171–177.

15. Ye Y, Ellenberg RM, Graham KE, Wigginton KR. Survivability, partitioning, and recovery of enveloped viruses in untreated municipal wastewater. Environmental science & technology. 2016. pp. 5077–5085.

16. Wu F, Xiao A, Zhang J, Gu X, Lee WL, Kauffman K, et al. SARS-CoV-2 titers in wastewater are higher than expected from clinically confirmed cases. medRxiv. 2020.

17. Hata A, Honda R. Potential Sensitivity of Wastewater Monitoring for SARS-CoV-2: Comparison with Norovirus Cases. Environmental Science & Technology. 2020.

18. Ibrahim NK. Epidemiologic surveillance for controlling Covid-19 pandemic: types, challenges and implications. Journal of Infection and Public Health. 2020;13: 1630–1638. doi:10.1016/j.jiph.2020.07.019

19. Medema G, Been F, Heijnen L, Petterson S. Implementation of environmental surveillance for SARS-CoV-2 virus to support public health decisions: Opportunities and challenges. Current Opinion in Environmental Science & Health. 2020.

20. Bibby K, Peccia J. Identification of viral pathogen diversity in sewage sludge by metagenome analysis. Environmental science & technology. 2013. pp. 1945–1951.

21. Gundy PM, Gerba CP, Pepper IL. Survival of coronaviruses in water and wastewater. Food and Environmental Virology. 2009. p. 10.

22. Lago PM, Gary Jr HE, Pérez LS, Cáceres V, Olivera JB, Puentes RP, et al. Poliovirus detection in wastewater and stools following an immunization campaign in Havana, Cuba. International journal of epidemiology. 2003. pp. 772–777.

23. Plante JA, Liu Y, Liu J, Xia H, Johnson BA, Lokugamage KG, et al. Spike mutation D614G alters SARS-CoV-2 fitness. Nature. 2020; 1–6.

24. Quick J, Grubaugh ND, Pullan ST, Claro IM, Smith AD, Gangavarapu K, et al. Multiplex PCR method for MinION and Illumina sequencing of Zika and other virus genomes directly from clinical samples. Nat Protoc. 2017;12: 1261–1276. doi:10.1038/nprot.2017.066

25. Hoenen T, Groseth A, Rosenke K, Fischer RJ, Hoenen A, Judson SD, et al. Nanopore sequencing as a rapidly deployable Ebola outbreak tool. Emerging infectious diseases. 2016. p. 331.

26. Medema G, Been F, Heijnen L, Petterson S. Implementation of environmental surveillance for SARS-CoV-2 virus to support public health decisions: Opportunities and challenges. Current Opinion in Environmental Science & Health. 2020.

27. Bivins A, Greaves J, Fischer R, Yinda KC, Ahmed W, Kitajima M, et al. Persistence of SARS-CoV-2 in water and wastewater. Environmental Science & Technology Letters. 2020.

28. Corpuz MVA, Buonerba A, Vigliotta G, Zarra T, Ballesteros Jr F, Campiglia P, et al. Viruses in wastewater: occurrence, abundance and detection methods. Science of the Total Environment. 2020. p. 140910.

29. Naddeo V, Liu H. Editorial Perspectives: 2019 novel coronavirus (SARS-CoV-2): what is its fate in urban water cycle and how can the water research community respond? Environmental Science: Water Research & Technology. 2020. pp. 1213–1216.

30. Sharif S, Ikram A, Khurshid A, Salman M, Mehmood N, Arshad Y, et al. Detection of SARS-Coronavirus-2 in wastewater, using the existing environmental surveillance network: An epidemiological gateway to an early warning for COVID-19 in communities. MedRxiv. 2020.

31. Urban Volume – Central Bureau of Statistics. [cited 14 Mar 2021]. Available: https://cbs.gov.np/urban-volume/

32. QGIS Desktop. In: OSGeo [Internet]. [cited 14 Mar 2021]. Available: https://www.osgeo.org/projects/qgis/

33. OpenStreetMap contributors. Planet dump retrieved from https://planet.osm.org. 2017.

34. Michael-Kordatou I, Karaolia P, Fatta-Kassinos D. Sewage analysis as a tool for the COVID-19 pandemic response and management: the urgent need for optimised protocols for SARS-CoV-2 detection and quantification. Journal of Environmental Chemical Engineering. 2020;8: 104306. doi:10.1016/j.jece.2020.104306

35. Randazzo W, Truchado P, Cuevas-Ferrando E, Simón P, Allende A, Sánchez G. SARS-CoV-2 RNA in wastewater anticipated COVID-19 occurrence in a low prevalence area. Water Research. 2020. p. 115942.

36. Farkas K, McDonald JE, Malham SK, Jones DL. Two-step concentration of complex water samples for the detection of viruses. Methods and protocols. 2018;1: 35.

37. BioRender. [cited 7 Mar 2021]. Available: https://app.biorender.com/gallery

38. BioRender. In: BioRender [Internet]. [cited 14 Mar 2021]. Available: https://biorender.com/

39. Quan P-L, Firth C, Street C, Henriquez JA, Petrosov A, Tashmukhamedova A, et al. Identification of a severe acute respiratory syndrome coronavirus-like virus in a leaf-nosed bat in Nigeria. MBio. 2010;1.

40. De Coster W, D'Hert S, Schultz DT, Cruts M, Van Broeckhoven C. NanoPack: visualizing and processing long-read sequencing data. Berger B, editor. Bioinformatics. 2018;34: 2666–2669. doi:10.1093/bioinformatics/bty149

41. Wick R. Porechop. Github https://github com/rrwick/Porechop. 2017.

42. Release Filtlong v0.2.0 · rrwick/Filtlong. In: GitHub [Internet]. [cited 16 Mar 2021]. Available: /rrwick/Filtlong/releases/tag/v0.2.0

43. Koren S, Walenz BP, Berlin K, Miller JR, Bergman NH, Phillippy AM. Canu: scalable and accurate long-read assembly via adaptive *k* -mer weighting and repeat separation. Genome Res. 2017;27: 722–736. doi:10.1101/gr.215087.116

44. Altschul SF, Gish W, Miller W, Myers EW, Lipman DJ. Basic local alignment search tool. J Mol Biol. 1990;215: 403–410. doi:10.1016/S0022-2836(05)80360-2

45. Quick J. nCoV-2019 sequencing protocol v3 (LoCost) V.3. University of Birmingham; 2020 Aug. Available: https://www.protocols.io/view/ncov-2019-sequencing-protocol-v3-locost-bh42j8ye

46. artic-network/rampart. ARTICnetwork; 2021. Available: https://github.com/artic-network/rampart

47. ARTIC: a bioinformatics pipeline for working with virus sequencing data sequenced with nanopore. In: GitHub [Internet]. [cited 31 Jan 2021]. Available: https://github.com/artic-network/fieldbioinformatics

48. Loman N, Rowe W, Rambaut A. nCoV-2019 novel coronavirus bioinformatics protocol. Artic Network. 2020.

49. Li H. Minimap2: pairwise alignment for nucleotide sequences. Birol I, editor. Bioinformatics. 2018;34: 3094–3100. doi:10.1093/bioinformatics/bty191

50. Li H, Handsaker B, Wysoker A, Fennell T, Ruan J, Homer N, et al. The Sequence Alignment/Map format and SAMtools. Bioinformatics. 2009;25: 2078–2079. doi:10.1093/bioinformatics/btp352

51. czbiohub/sc2-illumina-pipeline. Chan Zuckerberg Biohub; 2021. Available: https://github.com/czbiohub/sc2-illumina-pipeline

52. Singer J, Gifford R, Cotten M, Robertson D. CoV-GLUE: a web application for tracking SARS-CoV-2 genomic variation. 2020.

53. Introduction to waterfall plots | Griffith Lab. [cited 12 Mar 2021]. Available: https://genviz.org/module-03-genvisr/0003/02/01/waterfall_GenVisR/

54. Mercatelli D, Giorgi FM. Geographic and genomic distribution of SARS-CoV-2 mutations. Frontiers in microbiology. 2020;11: 1800.

55. Skidmore ZL, Wagner AH, Lesurf R, Campbell KM, Kunisaki J, Griffith OL, et al. GenVisR: genomic visualizations in R. Bioinformatics. 2016;32: 3012–3014.

56. Boni MF, Lemey P, Jiang X, Lam TT-Y, Perry BW, Castoe TA, et al. Evolutionary origins of the SARS-CoV-2 sarbecovirus lineage responsible for the COVID-19 pandemic. Nature Microbiology. 2020;5: 1408–1417.

57. Matyášek R, Kovařík A. Mutation patterns of human SARS-CoV-2 and bat RaTG13 coronavirus genomes are strongly biased towards C> U transitions, indicating rapid evolution in their hosts. Genes. 2020;11: 761.

58. GISAID - Initiative. [cited 29 Mar 2021]. Available: https://www.gisaid.org/

59. Douglas T, Young M. Virus particles as templates for materials synthesis. Advanced Materials. 1999;11: 679–681.

60. Recombination, Reservoirs, and the Modular Spike: Mechanisms of Coronavirus Cross-Species Transmission | Journal of Virology. Available: https://jvi.asm.org/content/84/7/3134

652 61. Rambaut A, Holmes EC, O'Toole Á, Hill V, McCrone JT, Ruis C, et al. A dynamic nomenclature
653 proposal for SARS-CoV-2 lineages to assist genomic epidemiology. Nature microbiology. 2020;5:
654 1403–1407.

655 62. Chen J, Wang R, Wang M, Wei G-W. Mutations strengthened SARS-CoV-2 infectivity. Journal of
656 molecular biology. 2020;432: 5212–5226.

657 63. Singh A, Steinkellner G, Köchl K, Gruber K, Gruber CC. Serine 477 plays a crucial role in the
658 interaction of the SARS-CoV-2 spike protein with the human receptor ACE2. Scientific reports.
659 2021;11: 1–11.

660 64. CDC. Coronavirus Disease 2019 (COVID-19). In: Centers for Disease Control and Prevention
661 [Internet]. 11 Feb 2020 [cited 14 Mar 2021]. Available: https://www.cdc.gov/coronavirus/2019-
662 ncov/more/science-and-research/scientific-brief-emerging-variants.html

663 65. Mahase E. Covid-19: What do we know about the late stage vaccine candidates? British Medical
664 Journal Publishing Group; 2020.

665 66. COVID T. An integrated national scale SARS-CoV-2 genomic surveillance network. The Lancet
666 Microbe. 2020.

667

668 **S1 Table: Blast result analysis of Coronavirus origin from sewage samples of Pilot phase**
669 **study**

Sample sites	Query ID	Accession	Organism	Evalue	Seqlen	Querycov	Identity
TH1	tig00000001	AL158839.11	Human	1.00E-119	788	86	99.6
	tig00000002	KT254285.1	Duck-dominant coronavirus	0	480	99	96.26
	tig00000003	KF293666.1	Human coronavirus 229E	4.00E-78	466	44	92.96
	tig00000004	MT655131.1	SARS-CoV-2	0	472	92	98.17
	tig00000005	KF294370.1	Rat cov	0	471	100	90.87
	tig00000006	MN306040.1	Human coronavirus NL63	0	391	100	99.49
	tig00000007	no significant hits					
Te3	tig00000001	LR824127.1	SARS-CoV-2	0	422	96	95.82
	tig00000001	KT254285.1	Duck-dominant coronavirus	0	466	100	96.15
	tig00000002	KF294370.1	Rat cov	2.00E-123	316	99	92.04
	tig00000003	no significant hits					
	tig00000004	no significant hits					
TH2	tig00000001	KT254285.1	Duck-dominant coronavirus	0	475	99	96.2
	tig00000002	KF294370.1	Rat cov	1.00E-125	327	99	91.38
APF	tig00000001	MT628184.1	SARS-CoV-2	3.00E-153	319	99	98.73

670

671 **S2 Table: Real time PCR data, viral load and population distribution of different sites.**
672 **Amplified genes- envelope (E), internal control (house-keeping gene, IC), RdRp and**
673 **nucleoplasmid (N) genes.**

S.N.	Date	Sampling Site	RT-PCR Result (Ct value)				Viral Load (viral copies per ml)	Est. human pop. Community
			E gene	IC	RdRp	N gene		
1.	26/7/2020	BA-1	-	-	35	-	-	1486
2.	26/7/2020	BA-2	20.1	-	-	-	-	518
3.	26/7/2020	BA-3	-	-	-	36.4	-	636
4.	10/09/2020	GW13	33.9	33.5	36.1	35.5	2090	Unknown
5.	27/09/2020	GW10	32.9	29.9	37.3	34.7	1,950	532
6.	4/10/2020	GW7	36.2	-	-	34.5	-	330
7.	9/11/2020	GW11	25.9	27.6	29.5	27.5	242000	2367
8.	11/11/2020	GW14	28.0		30.1	28.4	43100	Unknown
9.	12/11/2020	SA1	34.0	35.6	36.2	33.8	295	286
10.	18/11/2020	SA2	29.0	30.5	30.5	29.6	28900	81
11.	19/11/2020	SA7	27.5	30.5	32.2	29.1	7840	756
12.	20/11/2020	CH4	30.6	30.3	33	31.0	3640	700
13.	22/11/2020	KU1	28.0	29.6	30.8	28.4	92,300	1686
14.	23/11/2020	SA6	32.3	-	34.7	32.0	321	101
15.	24/11/2020	SA5	27.8	30.2	28.8	28.1	60,400	400
16.	25/11/2020	SA4	28.4	30.6	34.2	29.8	2820	204
17.	26/11/2020	SA3	30.2	28.6	34.3	30.6	1640	191
18.	27/11/2020	SA9	30.4	28.6	33.7	31.1	2390	227
19.	30/11/2020	GW12	29	30.9	-	29.4	-	Unknown
20.	1/12/2020	GW15	32.7	26.3	33.1	32.6	3660	Unknown

674

675 **S3 Table: AMPure bead clean up and DNA quantification data of pool1 & pool2 artic PCR**
676 **products in positive sewage samples before Indexing (Pilot study)**

677

S.N.	Sample ID	ng of DNA present	Size of PCR product	Femtomoles of DNA present	Femtomoles of DNA required	ng of DNA required	Volume of DNA required	Volume of water required
1	PL_1_Env5	4.86	400	18.72	200	51.92	10.7	39.3
2	PL_1_Env10	0.85	400	3.27	200	51.92	60.7	-10.7
3	PL_1_E2	9.93	400	38.25	200	51.92	5.2	44.8
4	PL_2_Env5	2.45	400	9.44	200	51.92	21.2	28.8
5	PL_2_Env10	0.33	400	1.27	200	51.92	156.7	-106.7
6	PL_2_E2	0.51	400	1.96	200	51.92	102.7	-52.7
7	PL_1_env1	33.60	400	129.43	200	51.92	1.5	48.5
8	PL_1_env2	28.60	400	110.17	200	51.92	1.8	48.2
9	PL_2_env1	1.59	400	6.12	200	51.92	32.7	17.3
10	PL_2_env2	2.05	400	7.9	200	51.92	25.3	24.7

678 **S4 Table: AMPure bead clean up and DNA quantification data of pool1 & pool2 ARTIC PCR products in positive sewage**
679 **samples before indexing**

S.N.	SAMPLE ID	VOLUME	AMPURE BEAD	READING 1	READING 2	READING 3	Average	ng for 100 fm w/ 400bp	Vol. of DNA
1.	GW11 (P1)	19	26.6	13.2	13.3	13.3	13.27	25.96	2.0
2.	SA2 (P1)	19	26.6	5.48	5.48	5.5	5.49	25.96	4.7
3.	SA7 (P1)	19	26.6	8.96	8.96	9	8.97	25.96	2.9
4.	CH4 (P1)	38	53.2	2.02	2.02	2.02	2.02	25.96	12.9
5.	KU1 (P1)	19	26.6	6.08	6.08	6.08	6.08	25.96	4.3
6.	SA5 (P1)	19	26.6	8.1	8.1	8.12	8.11	25.96	3.2
7.	GW11 (P2)	19	26.6	10.1	10.1	10.1	10.10	25.96	2.6
8.	SA2 (P2)	19	26.6	6.58	6.6	6.6	6.59	25.96	3.9
9.	SA7 (P2)	19	26.6	3.98	4	4	3.99	25.96	6.5
10.	CH4 (P2)	38	53.2	8.9	8.92	8.94	8.92	25.96	2.9
11.	KU1 (P2)	19	26.6	6.72	6.72	6.74	6.73	25.96	3.9
12.	SA5 (P2)	19	26.6	8.1	8.1	8.1	8.10	25.96	3.2
13.	GW10(P1)	20	28	1.02	1.03	1.04	1.03	25.96	25.0
14.	GW13(P1)	20	28	1.3	1.3	1.31	1.30	25.96	19.8
15.	GW14(P1)	20	28	16.2	16.3	16.3	16.26	25.96	1.6
16.	SA1(P1)	20	28	0.474	0.46	0.452	0.46	25.96	57.4
17.	SA6(P1)	20	28	4.16	4.18	4.2	4.18	25.96	6.2
18.	SA4(P1)	20	28	9.9	9.92	9.94	9.92	25.96	2.6
19.	SA3(P1)	20	28	0.448	0.45	0.452	0.45	25.96	57.4
20.	SA9(P1)	20	28	3.9	3.9	3.92	3.91	25.96	6.6
21.	GW12(P1)	20	28	3.5	3.5	3.52	3.51	25.96	7.4
22.	GW15(P1)	20	28	36	36	36	36	25.96	0.7
23.	GW10(P2)	20	28	1.06	1.07	1.07	1.06	25.96	24.3
24.	GW13(P2)	20	28	4.14	4.14	4.14	4.14	25.96	6.3
25.	GW14(P2)	20	28	24.6	24.6	24.6	24.6	25.96	1.1
26.	SA1(P2)	20	28	0.936	0.936	0.938	0.94	25.96	27.7
27.	SA6(P2)	20	28	3.6	3.2	2.92	3.24	25.96	8.9
28.	SA4(P2)	20	28	11.9	11.9	11.6	11.8	25.96	2.2
29.	SA3(P2)	20	28	6.28	6.28	6.28	6.28	25.96	4.1
30.	SA9(P2)	20	28	4.22	4.22	4.24	4.22	25.96	6.1
31.	GW12(P2)	20	28	8.24	8.24	8.26	8.24	25.96	3.1
32.	GW15(P2)	20	28	4.36	4.36	4.36	4.36	25.96	6.0

680